ACS APPLIED MATERIALS & INTERFACES

Forum Article

www.acsami.org

Increased Tensile Strength of Carbon Nanotube Yarns and Sheets through Chemical Modification and Electron Beam Irradiation

Sandi G. Miller,*[,†] Tiffany S. Williams,[†] James S. Baker,[‡] Francisco Solá,[†] Marisabel Lebron-Colon,[†] Linda S. McCorkle,[†,⊥] Nathan G. Wilmoth,[§] James Gaier,[†] Michelle Chen,[†,∥] and Michael A. Meador[†]

[†]NASA Glenn Research Center, 21000 Brookpark Road, Cleveland, Ohio 44135, United States

[‡]Oak Ridge Associated Universities, 21000 Brookpark Road, Cleveland, Ohio 44135, United States

[§]Vantage Partners, LLC, 21000 Brookpark Road, Cleveland, Ohio 44135, United States

[⊥]Ohio Aerospace Institute, Cleveland, Ohio 44135, United States

Supporting Information

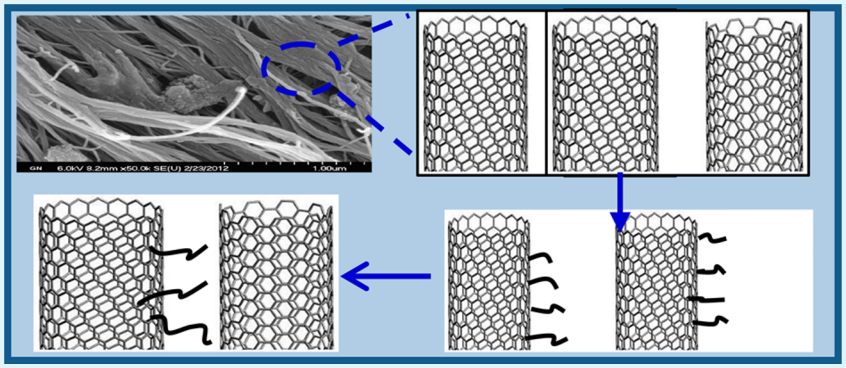

ABSTRACT: The inherent strength of individual carbon nanotubes (CNTs) offers considerable opportunity for the development of advanced, lightweight composite structures. Recent work in the fabrication and application of CNT forms such as yarns and sheets has addressed early nanocomposite limitations with respect to nanotube dispersion and loading and has pushed the technology toward structural composite applications. However, the high tensile strength of an individual CNT has not directly translated into that of sheets and yarns, where the bulk material strength is limited by intertube electrostatic attractions and slippage. The focus of this work was to assess postprocessing of CNT sheets and yarns to improve the macroscale strength of these material forms. Both small-molecule functionalization and electron-beam irradiation were evaluated as means to enhance the tensile strength and Young's modulus of the bulk CNT materials. Mechanical testing revealed a 57% increase in tensile strength of CNT sheets upon functionalization compared with unfunctionalized sheets, while an additional 48% increase in tensile strength was observed when functionalized sheets were irradiated. Similarly, small-molecule functionalization increased tensile strength of yarn by up to 25%, whereas irradiation of the functionalized yarns pushed the tensile strength to 88% beyond that of the baseline yarn.

KEYWORDS: *carbon nanotube, tensile strength, functionalization, electron-beam irradiation, cross-link, focused ion beam*

INTRODUCTION

Nanocomposite technology provides a means to reduce the weight of composite structures through increased material performance and an accompanying reduction of part thickness requirements. Individual single-walled carbon nanotubes (SWCNTs) have been widely investigated for weight reduction in aerospace structures because of the theoretical tensile strength of 75−135 GPa for an individual SWCNT and measured tensile strengths of up to 100 GPa.[1−3] Unfortunately, upon dispersion in a matrix, the impressive mechanical properties of individual tubes have not translated to a significant increase in polymer/CNT nanocomposite strength. Nanocomposites based on CNT dispersion generally contain low nanotube loadings (typically on the order of a few weight percent) because of agglomeration at higher concentrations, and they rely on the formation of CNT networks and interface optimization for translation of properties to the bulk material. To address the performance challenges posed by dispersion, processes to increase the CNT content in a resin or composite have been reported and include the incorporation of fuzzy fiber or CNT mat interleaves.[4,5]

Special Issue: Applications of Hierarchical Polymer Materials from Nano to Macro

Received: December 17, 2013
Accepted: March 28, 2014
Published: April 10, 2014

Recent focus has moved toward the fabrication of CNT sheets and yarns with projected applications as drop-in replacements for carbon fiber in composite structures. In such a material, the mechanical load would be carried by the macro-scale CNT reinforcements, and the dependence of the nanocomposite properties on the interfacial strength would be reduced.[6] Recently, companies such as Nanocomp Technologies, Inc. (Concord, NH) and General Nano (Cincinnati, OH) have commercialized sheets and yarns produced by dry spinning of CNT aerogels and vertically aligned CNT arrays. The tensile strength of the CNT sheets and yarns is limited by van der Waals forces; however, the yarn specific strength is generally greater because of tube alignment and entanglement generated in the spinning process. The inherent limitation of macro-scale CNT material strength resides in weak intratube (shell to shell) and intertube shear interactions. Therefore, increasing the material strength at both of these levels is crucial to the development of high-strength CNT material forms.[7,8] Several groups have investigated procedures to introduce covalent bonds both between CNT shells and between adjacent CNTs. Cornwell and Welch reported molecular dynamics simulations of SWCNT bundles revealing that tensile strengths as high as 62 GPa could be achieved through cross-linking between tubes in the bundle.[9] Theoretical studies by Huhtala and co-workers on double-walled CNTs (DWCNTs) indicated that the introduction of a small number of defects (cross-links) increases the force required to initiate sliding between nanotube shells from 0.1−0.4 nN to as much as 4−8 nN.[10] Naraghi and co-workers reported nanomechanical shear experiments between functionalized bundles of CNTs combined with multiscale simulations to reveal the mechanistic and quantitative role of nanotube surface functionalization on CNT−CNT interactions.[11]

Several publications have identified electron-beam (e-beam) irradiation as a feasible mechanism to induce cross-linking between CNT bundles and limit shear failure.[7−16] Building on prior experimental and theoretical work done on multiwalled CNTs (MWCNTs),[1,2] Espinosa and co-workers experimentally demonstrated up to a 16-fold enhancement of the mechanical performance (modulus and strength) of DWCNT bundles following high-energy e-beam irradiation in situ via transmission electron microscopy (TEM). They attributed the increase to a combination of both intra- and intertube cross-linking. The nature of the cross-linking was deduced by directly imaging the fracture surfaces of CNT bundles: lightly cross-linked bundles showed a sword-in-sheath type of failure, while highly cross-linked bundles exhibited complete fracture.[7] The results confirmed atomistic modeling reported in the literature.[9]

Work carried out at Florida State University investigated the effects of e-beam irradiation on the properties of SWCNT membranes. E-beam irradiation was carried out at a commercial facility under atmospheric conditions. The irradiation dosage varied from 9.2×10^{15} to 2.8×10^{17} e/cm^2, and the result was a 6-fold increase in the membrane tensile strength.[12,13] Duchamp et al.[14] measured an increase in the bending modulus of vapor-grown CNTs following e-beam irradiation. While an initial increase in modulus was observed, longer irradiation times led to a reduction in modulus. This was attributed to damage to the tubes after extended irradiation times.

While these studies have demonstrated an increase in tensile strength and modulus, further increases in the mechanical properties of CNT sheets and yarns are necessary before they can perform as suitable replacements for conventional intermediate-modulus carbon fiber. We have investigated the combined effects of small-molecule functionalization and e-beam-generated cross-linking in an attempt to further increase the tensile properties of CNT sheets and yarns. Herein we present the results of these studies.

EXPERIMENTAL SECTION

Materials. CNT yarn was purchased from Nanocomp Technologies (batch 5279-7) and was produced through a proprietary process. The as-received yarn was acetone-condensed at Nanocomp Technologies and was binder-free. The vendor reported the specific tensile strength of this yarn as 0.51 N/tex, and the average diameter, as measured at NASA Glenn Research Center, was 65 μm. CNT sheets were purchased from Nanocomp Technologies (batch 5333) as an untreated and unwashed form of the sheet. The CNT sheets were produced by depositing a CNT aerogel onto a rotating drum. As a result, they exhibited anisotropy with respect to tensile strength. The tensile properties reported in this paper were measured in the direction of drum rotation (0° direction).

Small-Molecule Functionalization. Functional groups were grafted onto the CNTs via nitrene chemistry using a modification of literature procedures.[17] 2-Hydroxyethyl and 3-aminopropyl functionalities were chosen with an eye toward utilizing the pendant −OH and $-NH_2$ groups as reaction sites to bond to epoxy monomers.

3-Aminopropyl-Functionalized CNT Sheets. 3-Aminopropyl-functionalized nanotubes were prepared by reaction with 3-azidopropane-1-amine in a modification of a literature procedure,[17] as in the following example. 3-Azidopropane-1-amine (0.24 g, 2.4 mmol) in 0.75 mL of *N*-methylpyrrolidone was added to a section of CNT sheet (57.8 mg, ∼4.8 mmol of carbon atoms) in a round-bottom flask equipped with a condenser, followed by heating at 180 °C under a N_2 atmosphere for 18 h. The sample was washed by sequential Soxhlet extractions in dimethyl formamide (DMF), water, and acetone (5, 18, and 2 h, respectively) and then dried under vacuum at 45 °C to yield 63.7 mg of functionalized sheet material (∼1.7 mol % functionality based upon mass increase).

2-Hydroxyethyl-Functionalized CNT Sheets. 2-Hydroxyethyl-functionalized nanotubes were prepared by reaction with 2-azidoethanol in a modification of a literature procedure,[17] as in the following example. 2-Azidoethanol (0.70 g, 8.05 mmol) was added to a section of CNT sheet (28.4 mg, ∼2.4 mmol of carbon atoms) in a round-bottom flask equipped with a condenser, followed by heating at 180 °C under a N_2 atmosphere for 20 h. The sample was washed by sequential Soxhlet extractions in DMF, water, and acetone (8 h each) and then dried under vacuum at 45 °C to yield 33.5 mg of functionalized sheet material (∼3.8 mol % functionality based upon mass increase).

Throughout the functionalization procedure, the sheets were fully wetted out by solution. Raman spectroscopy of the sheet outer surfaces revealed comparable I_G/I_D ratios indicative of functionalization at these sites. The through-thickness functionalization was not evaluated.

Electron-Beam Irradiation. Irradiation experiments were performed at the Mercury Plastics e-beam facility in Middlefield, OH. This manufacturing environment was utilized to accommodate the large volume of material necessary for this effort and future subcomponent fabrication. As a result, a vacuum or inert gas atmosphere was not available, and irradiation was carried out in air.

CNT materials were bound to a water-cooled aluminum plate and exposed to e-beam fluxes ranging from 4.8×10^{16} to 2.2×10^{17} e/cm^2, which corresponded to irradiation times varying between 20 and 90 min. A beam current of 36 mA was used, and the CNT sheets and yarns were irradiated at 2 MeV under atmospheric conditions. The irradiated materials included (1) as-received sheet and yarn, (2) 2-hydroxyethyl-functionalized sheet and yarn, and (3) 3-aminopropyl-functionalized sheet and yarn.

Tensile Strength Measurements. A minimum of five tensile test coupons were cut from the parent sheet or yarn material. The coupons were measured to be 2.54 cm long × 0.64 cm wide for the CNT sheet and 2.54 cm long for the CNT yarn specimens. Tensile tests were

dx.doi.org/10.1021/am4058277 | ACS Appl. Mater. Interfaces 2014, 6, 6120−6126

performed on a Tytron 250 MicroTester testing system using a 22 N load cell and cross-head speeds of 10 mm/min with the sheet and 7.5 mm/min with the yarn. The CNT materials were mounted on card stock, and the mount was speckle-painted for digital image correlation. The strength and modulus values of the sheets were normalized by volumetric density, whereas the yarn data were normalized by linear density.

Spectroscopic Characterization. Raman spectroscopy was performed using a Renishaw System 2000 Raman microscope with a 514 nm argon ion laser excitation source. The integrated intensities of the G and D bands were calculated using OMNIC software, and I_G/I_D ratios are reported as averages of measurements taken from 10 locations on the CNT samples. X-ray photoelectron spectroscopy (XPS) measurements were performed on a PHI 5000 Versaprobe (ULVAC-PHI) spectrometer using monochromatic microfocused Al X-rays (200 μm, 43.4 W) with a photoelectron takeoff angle of 45°. A dual-beam charge neutralizer (7 V Ar^+ beam and 30 V electron beam) was used to minimize surface charging. The base pressure of the main chamber ($<1 \times 10^{-7}$ Pa) was achieved by evacuation using turbomolecular and ion-getter pumps. Survey scans using a 117.4 eV pass energy were taken initially to identify all of the trace components and to calculate atomic concentrations. Higher-resolution carbon, oxygen, and nitrogen scans for individual regions were then obtained using a pass energy of 11.75 eV.

Electron Microscopy. Cross-section imaging of CNT yarns was conducted in an Auriga focused ion beam (FIB) microscope from Carl Zeiss. The Auriga microscope is a crossed-beam FIB instrument in which a gallium beam is used for milling procedures and the electron beam column is used for image formation. All of the images were acquired using an In lens and secondary electrons at beam energies of 5 keV. Milling procedures involved the formation of a trench in the CNT yarns using an ion beam current of 2 nA at 30 kV followed by 600 pA at 30 kV of the imaged surface. All other scanning electron microscopy (SEM) images were taken with a Hitachi S4700 microscope operated at 5–6 keV.

RESULTS AND DISCUSSION

The structure and morphology of the as-received CNT sheets and yarns were characterized by SEM (Figures 1–3). The SEM images in Figures 1 and 2 indicate that the CNT sheets were

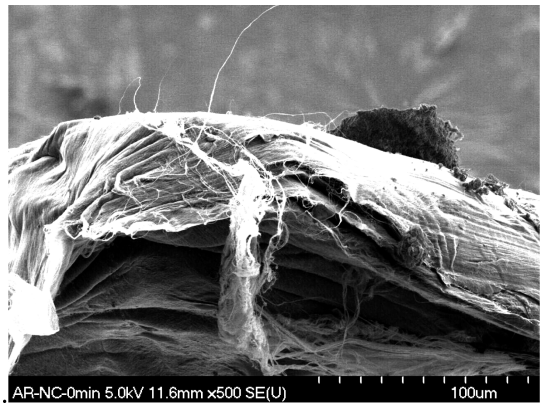

Figure 1. SEM image of an as-received CNT sheet edge, showing multiple layers within the single sheet.

composed of semialigned nanotubes residing within a stack of multiple layers. The sheet layers were easily delaminated prior to functionalization, where they were condensed through solvent wet-out. While considerable catalyst and amorphous carbon content was observed, sheet purification was not part of this initial effort, and the influence of catalyst removal on the mechanical properties is being evaluated in a parallel study. A significant level of porosity was seen within the CNT sheets, as

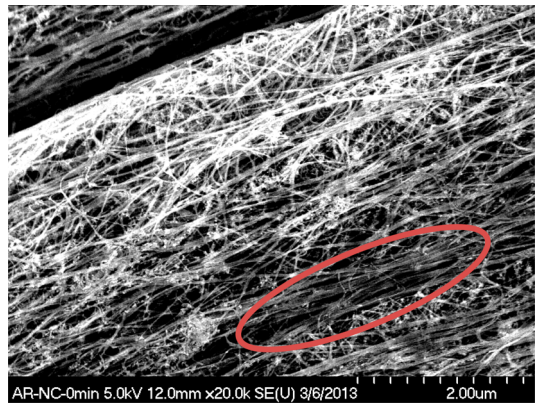

Figure 2. SEM image of a CNT sheet, showing high catalyst content and a preferred order of alignment.

indicated by the dark regions between tube filaments (Figure 2). Physical postprocessing methods such as densification and prestrain to reduce the void space within the sheet are being evaluated and will be reported separately. While a macro-scale level of alignment was difficult to discern from the SEM images, localized alignment was observed throughout the material (Figure 2). Anisotropic behavior was noted from tensile test data of coupons cut at both 0° and 90° relative to the assumed alignment direction, as the tensile strength of coupons cut in the 0° direction was up to 50% higher than that of coupons cut in the 90° direction.

CNT yarn was fabricated through solid-state spinning of the same CNT aerogels used to produce the sheets. SEM images of the CNT yarn (Figure 3) show a network of wound nanotubes with considerable porosity between tube bundles. A significant amount of catalyst was distributed throughout the yarn.

The sheet thickness and yarn diameter varied throughout the test specimens. The average measured sheet thicknesses and yarn diameters for the tested samples are listed in Table 1.

CNT Sheet Cross-Linking by E-Beam Irradiation. E-beam irradiation conditions to induce cross-linking were chosen on the basis of data reported for irradiation of MWCNTs.[13] The intent of the irradiation study was a broad screening of exposure times and e-beam fluxes to measure the responses of both the as-received and functionalized CNT materials. The irradiation times and corresponding e-beam fluxes utilized in this study are outlined in Table 2.

The CNT sheets were characterized by Raman spectroscopy and XPS prior to and following e-beam irradiation. The I_G/I_D ratios measured by Raman spectroscopy and C/O ratios calculated from XPS are listed in Table 3. The Raman spectra of the as-received and functionalized sheet materials irradiated from 0 min through 90 min are supplied in the Supporting Information. Irradiation tended to decrease the I_G/I_D ratio, regardless of functionalization, as a result of a decrease in the intensity of the G band (~1570 cm^{-1}) and a corresponding increase in the intensity of the D band (1342 cm^{-1}). This trend was attributed to disruption of the pristine nanotubes' graphitic structure and conversion of nanotube sp^2-hybridized carbons to sp^3-hybridized ones by either intertube cross-linking or damage to the nanotubes. The Raman data were correlated with tensile test results to discern the effects of the e-beam on the material strength. The Raman data provided a clear trend of decreasing I_G accompanied by a steady increase in I_D with increasing irradiation time.

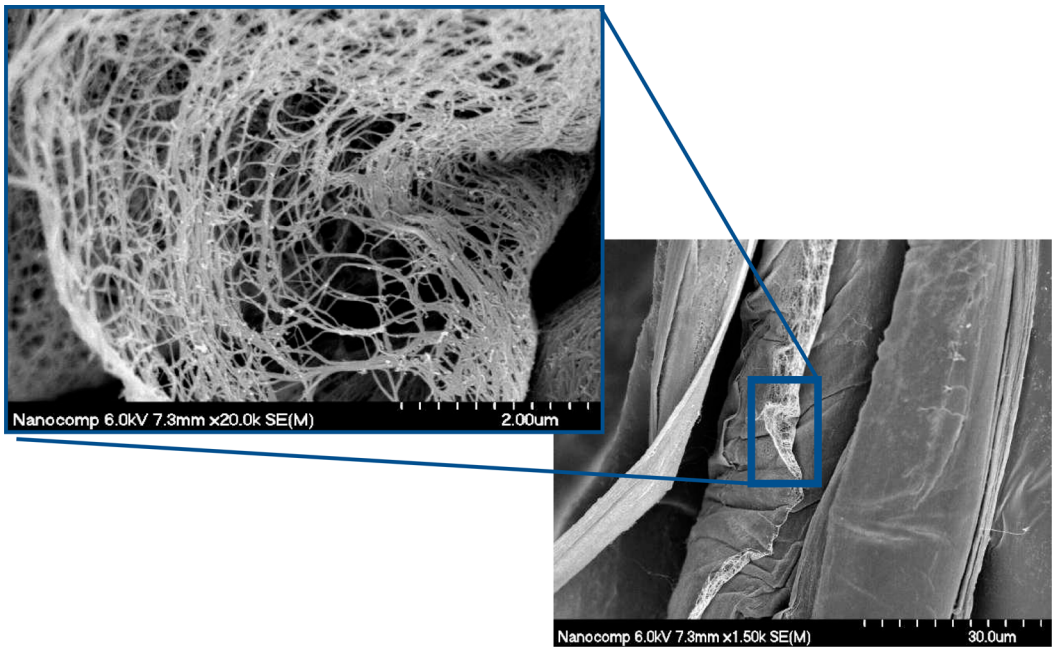

Figure 3. SEM images of as-received Nanocomp Technologies CNT yarn.

Table 1. Dimensions of Sheet and Yarn Tensile Coupons

	sheet thicknesses (μm)		
e-beam exposure time (min)	as-received	amine-functionalized	hydroxyl-functionalized
0	16.8 ± 3.1	18.0 ± 2.1	15.8 ± 2.9
20	20.0 ± 2.2	18.3 ± 2.1	18.7 ± 1.3
40	20.3 ± 2.6	15.4 ± 3.0	16.1 ± 1.9
90	20.5 ± 3.4	18.0 ± 1.8	17.0 ± 1.7
	yarn diameters (μm)		
e-beam exposure time (min)	as-received	amine-functionalized	hydroxyl-functionalized
0	67.0 ± 5.0	63.0 ± 5.4	66.7 ± 10.7
20	63.2 ± 8.3	66.3 ± 8.3	64.7 ± 6.7
40	62.2 ± 3.4	64.5 ± 3.7	73.6 ± 6.3
90	60.0 ± 4.8	65.8 ± 4.1	63.4 ± 5.0

Table 2. E-Beam Exposure Parameters

time (min)	beam current (mA)	fluence (e/cm^2)
20	36	4.8×10^{16}
40	36	9.6×10^{16}
90	36	2.2×10^{17}

Similarly, the Raman data for the irradiated 3-aminopropyl-functionalized sheets depict a steady reduction in I_G with increased irradiation. The Raman spectra of this material reflect hybridization within the CNT structure due to the functionalization process, as the I_G/I_D ratio at 0 min was smaller than that of the as-received material at 0 min irradiation (Table 3). The 3-aminopropyl-functionalized material showed the least reduction in I_G/I_D after 90 min of irradiation, which was attributed to cross-linking through the 3-aminopropyl functionalization sites.

The change in I_G/I_D following 2-hydroxyethyl functionalization was not statistically significant. This would suggest that functionalization may have favored reaction with amorphous carbon. As a result, I_G did not decrease until 90 min of irradiation.

XPS analysis revealed a reduction in the ratio of the carbon and oxygen peaks with increased irradiation time (Table 3). Because the e-beam irradiation was carried out in air, the reduction in the C/O ratio suggests the introduction of oxygen functionality into the CNTs due to the reaction of carbon-based free radicals with oxygen.[18]

Sheet Tensile Strength. The measured values of the specific tensile strength and modulus of the irradiated CNT sheets are shown in Figures 4 and 5, respectively. The strength of the as-received sheets was moderately increased with low irradiation (up to 40 min of exposure). However, a 30% decrease in tensile strength was measured following e-beam exposure of the as-received sheet for the full 90 min. This can be correlated with the Raman data, which showed a 25% decrease in I_G/I_D following 90 min of irradiation, and is indicative of damage to the CNT structure. Damage induced by radiation is due to carbon atom displacement, which effectively places a defect in the tube. Cross-linking at the defect will occur

Table 3. Summary of Raman and XPS Data for Sheet Materials with Increasing Irradiation Time

	unfunctionalized		amine-functionalized		hydroxyl-functionalized	
irradiation time (min)	I_G/I_D	C/O	I_G/I_D	C/O	I_G/I_D	C/O
0	3.0 ± 0.2	44.0	2.3 ± 0.2	23.4	3.3 ± 0.5	17.0
20	1.5 ± 0.5	37.2	1.7 ± 0.1	10.4	1.5 ± 0.1	10.5
40	1.7 ± 0.7	6.5	0.7 ± 0.1	6.5	1.3 ± 0.5	5.4
90	0.9 ± 0.2	9.6	1.4 ± 0.1	5.2	0.8 ± 0.1	4.8

dx.doi.org/10.1021/am4058277 | ACS Appl. Mater. Interfaces 2014, 6, 6120−6126

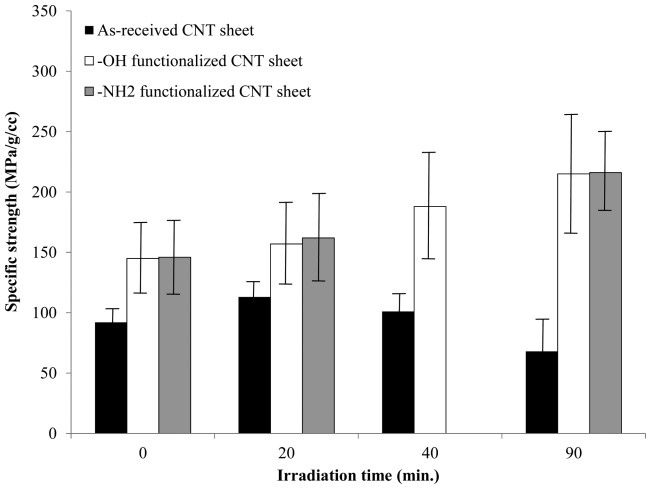

Figure 4. Specific tensile strength of small-molecule-functionalized CNT sheets upon e-beam exposure.

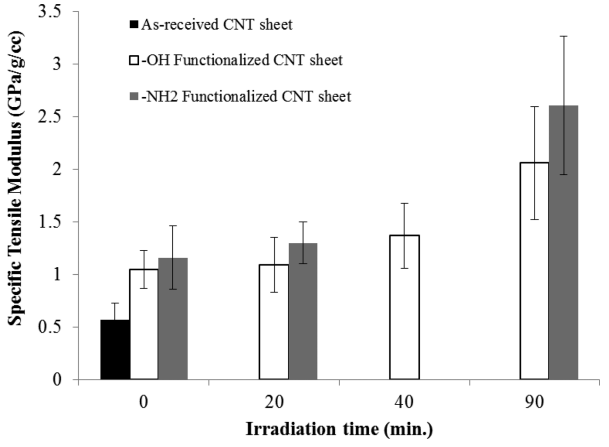

Figure 5. Specific tensile modulus of small-molecule-functionalized CNT sheets upon e-beam exposure.

only if these interstitial sites are sufficiently close to form covalent bonds. Otherwise, defects will continue to form, resulting in a CNT sheet of reduced strength. The data are in agreement with reports by Espinosa and co-workers[7] for DWCNTs and Wang[13] for MWCNTs, who observed damage to the CNTs and an accompanying loss of mechanical properties after prolonged e-beam irradiation.

The combined effect of functionalization and e-beam irradiation on the CNT sheet tensile strength can be seen in Figure 4. Prior to irradiation, both 2-hydroxyethyl and 3-aminopropyl functionalization served to increase the sheet tensile strength by ~15% relative to the as-received sheets as a result of hydrogen bonding between the pendant −OH or $-NH_2$ groups. In contrast to the unfunctionalized material, e-beam irradiation of the functionalized tubes for 90 min resulted in a 50% increase in sheet specific tensile strength. The improved tensile properties with functionalization in conjunction with the I_G/I_D trends suggest the formation of covalent bonds between the functionalized tubes. The net increase in sheet mechanical strength may be due to (a) greater reactivity of the 2-hydroxy and 2-aminopropyl groups toward e-beam irradiation or the CNT-centered radicals produced by e-beam irradiation and (b) the potential ability of the conformationally mobile alkyl groups to bridge the gaps between nanotubes and facilitate cross-linking. The influence of the small-molecule functionalization was significant in that it reversed the trend of mechanical property degradation with irradiation that had been seen in the baseline material. The preferential reactivity of the functional groups relative to the tubes themselves mitigates damage to the underlying CNT material and may allow the functional groups to serve as bridges to link neighboring tubes.

Cross-Linking of CNT Yarn by E-Beam Irradiation. The Raman data for functionalized and irradiated yarn are presented in Table 4. A significant reduction in I_G/I_D was recorded for the

Table 4. I_G/I_D Ratios Measured for CNT Yarn before and after Irradiation

sample	0 min	20 min	40 min	90 min
as-received	4.8 ± 1.7	1.7 ± 0.2	1.5 ± 0.1	1.0 ± 0.1
hydroxyl-functionalized	5.2 ± 1.6	1.6 ± 0.7	2.1 ± 0.2	1.4 ± 0.1
amine-functionalized	2.2 ± 0.8	2.4 ± 0.3	1.3 ± 0.1	1.1 ± 0.1

3-aminopropyl-functionalized yarn at 0 min of irradiation, and it was attributed to disruption of the sp^2 hybridization of the CNTs by the functionalization process. As with the sheet material, the 2-hydroxyethyl functionalization did not have an effect on I_G/I_D.

E-beam irradiation of the yarn generally decreased the I_G/I_D ratio, with the greatest decrease seen within the first 20 min of e-beam exposure. During this time, I_G considerably decreased with a corresponding increase in I_D. As will be seen in the mechanical test results, the Raman data support e-beam-induced cross-linking and subsequent increases in tensile strength.

The specific strength and specific modulus values of CNT yarns before and after e-beam irradiation are plotted in Figures 6 and 7, respectively. The large scatter in the tensile strength

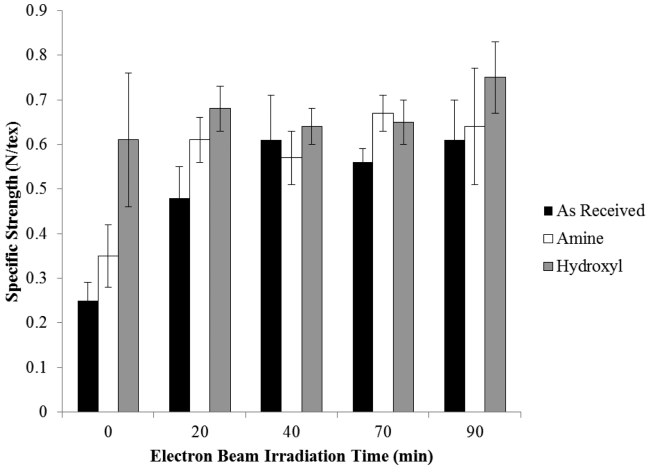

Figure 6. Specific tensile strength of as-received and functionalized CNT yarns upon e-beam irradiation.

values is due to significant variations in the diameter along the length of the yarn test specimen, although the error can be reduced through normalization by the linear density. Unlike CNT sheets, prolonged irradiation of CNT yarns did not result in a loss of tensile strength. In addition, e-beam irradiation tended to increase the yarn tensile strength to a greater extent relative to the sheet for the same exposure. For example, e-

dx.doi.org/10.1021/am4058277 | ACS Appl. Mater. Interfaces 2014, 6, 6120−6126

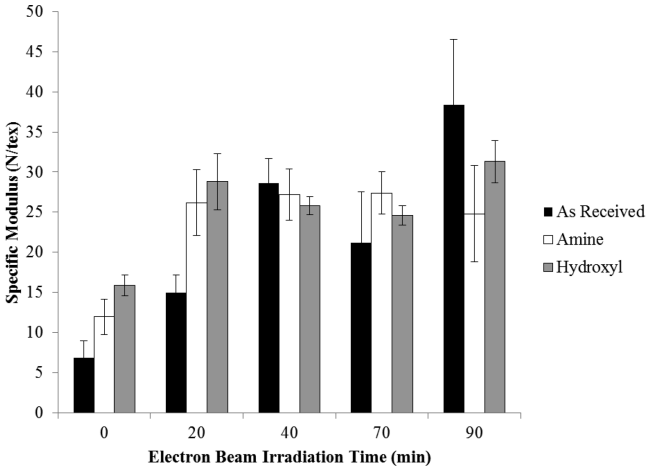

Figure 7. Specific tensile modulus of as-received and functionalized CNT yarns upon e-beam irradiation.

beam irradiation of the as-received material for 20 min led to a nominal strength increase of 25% in the CNT sheets and an 80% increase in yarn strength. Further irradiation (up to 90 min) led to a 240% increase in the tensile strength of the yarn, while the sheet strength was degraded under the same conditions. The improvement in tensile properties observed for the yarn in comparison to the sheet is attributed to the greater CNT alignment and entanglement inherent to the yarn structure, which increases the proximity of irradiation-induced dislocations and facilitates cross-linking. As with the sheet material, small-molecule functionalization benefited the tensile strength of the yarn. The enhancement of the strength was again most notable following 90 min of irradiation, where the specific strength of the 2-hydroxyethyl-functionalized yarn was increased 300% relative to the as-received material.

E-beam irradiation of the as-received yarns led to both a loss of ductility (strain-to-failure) and an increase in the modulus of the yarns, as evidenced by a reduction in the area under the stress−strain curves and an increase in slope, respectively. Representative stress−strain curves are shown in the Supporting Information. These changes are consistent with the formation of a cross-linked network within the yarn.[13]

FIB microscopy was employed to observe physical changes in the CNT yarns that might occur as a function of irradiation. A section of the yarn was etched to obtain a visual representation of irradiation-induced morphological changes to the yarn interior. An image of the interior morphology of the as-received yarn is provided in the Supporting Information.

FIB images obtained from e-beam-irradiated CNT yarns (Figure 8) suggest that the packing density of the nanotubes increased as a function of irradiation time, which is consistent with intertube cross-linking, the measured increase in tensile strength, and subsequent reduction in I_G/I_D. A decrease in the diameter of the as-received yarn with increased irradiation exposure was noted in Table 1, which would correspond to an increased packing density. The same trend was not observed in the functionalized materials, as the small-molecule functionalization provides a tethered moiety to facilitate cross-linking without increased packing density.

Most mechanisms proposed to explain the improvement in mechanical properties by intertube cross-linking rely on theoretical work that has been validated through experiments with isolated CNTs and isolated CNT bundles.[8] Cornwell and

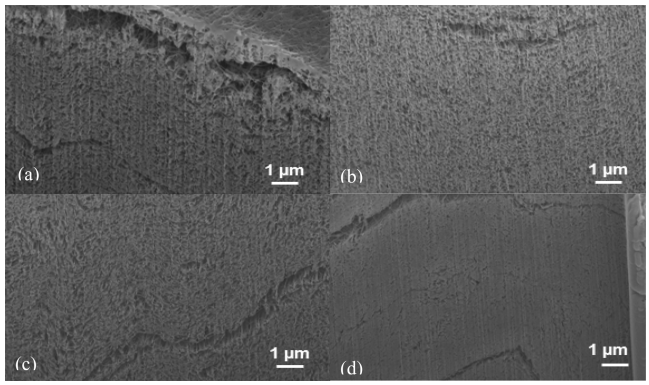

Figure 8. FIB microscopy images of the CNT yarn interior morphology following irradiation at (a) 0, (b) 20, (c) 40, and (d) 90 min.

Welch demonstrated theoretically that interstitials can promote cross-linking sites between several bundles within a fiber.[9] Therefore, we propose similar atomistic phenomena in the current study, where e-beam irradiation induces interstitial vacancies and leads to cross-linking.

CONCLUSIONS

The influence of small-molecule modification and e-beam irradiation on CNT sheet and yarn materials was evaluated. Both processes tended to reduce the I_G/I_D ratio due to disruption of the sp^2 hybridization of the pristine CNT material. This was attributed in most cases to intertube cross-link formation and supported by increased tensile strength. E-beam irradiation of an as-received, bulk CNT sheet material negatively impacted the material tensile strength upon exposure to an e-beam flux of 2.2×10^{17} e/cm^2 (90 min). However, the same exposure increased the specific strength of the functionalized materials by nearly 60%. Irradiation of the as-received yarn led to an increase in tensile strength through tube alignment and entanglement. Small-molecule functionalization provided a mechanism to increase the sheet tensile strength with or without e-beam exposure. Functionalization had less influence on the yarn structure with respect to increased tensile strength relative to the unmodified yarn.

ASSOCIATED CONTENT

Supporting Information

Raman spectra of e-beam-irradiated CNT samples, stress−strain curves, and an FIB microscopy image of the as-received yarn showing internal structure. This material is available free of charge via the Internet at http://pubs.acs.org.

AUTHOR INFORMATION

Corresponding Author

*E-mail: sandi.g.miller@nasa.gov.

Notes

The authors declare no competing financial interest.

[‖]NASA USRP Intern.

ACKNOWLEDGMENTS

This work was funded through the NASA Game Changing Development Program/Nanotechnology Project. J.S.B. was supported under the NASA Postdoctoral Program at the Glenn Research Center, administered by Oak Ridge Associated Universities through a contract with NASA. The authors

thank Dr. Jeffrey Eldridge for his assistance with Raman spectroscopy and Ms. Dorothy Lukco for her assitance with XPS.

REFERENCES

(1) Peng, B.; Locascio, M.; Zapol, P.; Li, S.; Mielke, S. L.; Schatz, G. C.; Espinosa, H. D. Measurements of Near-Ultimate Strength for Multi-Walled Carbon Nanotubes and Irradiation-Induced Crosslinking Improvements. *Nat. Nanotechnol.* **2008**, *3*, 626−631.
(2) Locascio, M.; Peng, B.; Zapol, P.; Zhu, Y.; Li, S.; Belytschko, T.; Espinosa, H. D. Tailoring the Load Carrying Capacity of MWCNTs through Inter-shell Atomic Bridging. *Exp. Mech.* **2009**, *49*, 169−182.
(3) Wang, M.-W; Goldberg, D.; Bando, Y. Tensile Tests on Individual Single-Walled Carbon Nanotubes: Linking Nanotube Strength with Its Defects. *Adv. Mater.* **2010**, *22*, 4071−4075.
(4) Wicks, S. S.; Kalamoun, S.; Williams, S.; Guzmán de Villoria, M.; Wardle, B. L. Effect of Manufacturing Route on Mode I Fracture Toughness of Aligned Carbon Nanotube Reinforced Composites. Presented at the 53nd AIAA Structures, Structural Dynamics, and Materials (SDM) Conference, Honolulu, Hawaii, 2012.
(5) Khan, S. U.; Kim, J.-K. Improved Interlaminar Shear Properties of Multiscale Carbon Fiber Composites with Bucky Paper Interleaves made from Carbon Nanofibers. *Carbon* **2012**, *50*, 5265−5277.
(6) Ma, W.; Liu, L.; Zhang, Z.; Yang, R.; Liu, G.; Zhang, T.; An, X.; Yi, X.; Ren, Y.; Niu, Z.; Li, J.; Dong, H.; Zhou, W.; Ajayan, P. M.; Xie, S. High-Strength Composite Fibers: Realizing True Potential of Carbon Nanotubes in Polymer Matrix through Continuous Reticulate Architecture and Molecular Level Couplings. *Nano Lett.* **2009**, *9*, 2855−2861.
(7) Filleter, T.; Bernal, R.; Li, S.; Espinosa, H. D. Ultrahigh Strength and Stiffness in Cross-Linked Hierarchical Carbon Nanotube Bundles. *Adv. Mater.* **2011**, *23*, 2855−2860.
(8) Wei, X.; Naraghi, M.; Espinosa, H. D. Optimal Length Scales Emerging from Shear Load Transfer in Natural Materials: Application to Carbon-Based Nanocomposite Design. *ACS Nano* **2012**, *6*, 2333−2344.
(9) Cornwell, C. F.; Welch, C. R. Very-High-Strength (60-GPa) Carbon Nanotube Fiber Design Based on Molecular Dynamics Simulations. *J. Chem. Phys.* **2011**, *134*, No. 204708.
(10) Huhtala, M.; Krasheninnikov, A. V.; Aittoneimi, J.; Stuart, S. J.; Nordlund, K.; Kaski, K. Improved Mechanical Load Transfer between Shells of Multi-Walled Carbon Nanotubes. *Phys. Rev. B* **2004**, *70*, No. 045404.
(11) Espinosa, H. D.; Filleter, T.; Naraghi, M. Multiscale Experimental Mechanics of Hierarchical Carbon-Based Material. *Adv. Mater.* **2012**, *24*, 2805−2823.
(12) Filleter, T.; Espinosa, H. D. Multi-scale Mechanical Improvement Produced in Carbon Nanotube Fibers by Irradiation Cross-linking. *Carbon* **2013**, *56*, 1−11.
(13) Wang, S. Functionalization of Carbon Nanotubes: Characterization, Modeling and Composite Applications. Ph.D. Thesis, Florida State University, Tallahassee, FL, 2006.
(14) Duchamp, M.; Meunier, R.; Smajda, R.; Mionic, M.; Magrez, A.; Seo, J. W.; Forro, L.; Song, B.; Tomanek, D. Reinforcing Multiwall Carbon Nanotubes by Electron Beam Irradiation. *J. Appl. Phys.* **2010**, *108*, No. 084314.
(15) Kis, A.; Csányi, G.; Salvetat, J.-P.; Lee, T.-N.; Couteau, E.; Kulik, A. J.; Benoit, W.; Brugger, J.; Forró, L. Reinforcement of Single-Walled Carbon Nanotube Bundles by Intertube Bridging. *Nat. Mater.* **2004**, *3*, 153−157.
(16) Xia, Z. H.; Guduru, P.; Curtin, W. A. Enhancing Mechanical Properties of Multiwall Carbon Nanotubes via sp^3 Interwall Bridging. *Phys. Rev. Lett.* **2007**, *98*, No. 245501.
(17) Gao, C.; He, H.; Zhou, L.; Zheng, X.; Zhang, Y. Scalable Functional Group Engineering of Carbon Nanotubes by Improved One-Step Nitrene Chemistry. *Chem. Mater.* **2009**, *21*, 360−370.
(18) Evora, M. C.; Klosterman, D.; Lafdi, K.; Li, L.; Abot, J. L. Functionalization of Carbon Nanofibers Through Electron Beam Irradiation. *Carbon* **2010**, *48*, 2037−2046.